Electronic Supplementary Information

Ultraselective Electrochemiluminescence Biosensor Based on Locked Nucleic Acid Modified Toehold-Mediated Strand Displacement Reaction and Junction-probe

Xi Zhang [a]**, Jing Zhang** [b]**, Dongzhi Wu** [a]**, Zhijing Liu** [a]**, Shuxian Cai** [a]**, Mei Chen** [a]**, Yanping Zhao** [a]**, Chunyan Li** [a]**, Huanghao Yang*** [c]**, Jinghua Chen*** [a]

a Department of Pharmaceutical Analysis, Faculty of Pharmacy, Fujian Medical University, Fuzhou, Fujian Province 350108, P R China.

b The Ministry of Education Key Laboratory of Biopesticide and Chemical Biology, and College of Life Sciences, Fujian Agriculture and Forestry University, Fuzhou, Fujian Province 350002, P R China.

c Ministry of Education Key Laboratory of Analysis and Detection for Food Safety, Fujian Provincial Key Laboratory of Analysis and Detection for Food Safety, Department of Chemistry, Fuzhou University, 350108 Fuzhou, P R China.

1. Experimental parts

Reagents. All oligonucleotides were synthesized by Sangong Biotech (Shanghai, China) Co., Ltd. and their base sequences were illustrated in Table S1. The concentrations were quantified by OD 260 based on their individual absorption coefficients, and all of them were HPLC purified. Tris-(hydroxymethyl) aminomethane(Tris) was purchased from Cxbio Biotechnology Co. Ltd. (Denmark). 6-Mercapto-1-hexano (97 %) (MCH), Hexaammineruthenium(℃) chloride (98 %) (RuHex), $Ru(bpy)_3^{2+}$ (99.95 %), $HAuCl_4$ and cysteamine ($SH-(CH_2)_2-NH_2$) were purchased from Sigma–Aldrich (USA). The buffer solutions were as follows: DNA immobilization buffer solution was 1.0 M NaCl–10mM Tris–1.0 mM

EDTA solution (pH 8.0). Hybridization buffer solution was 0.1 mM NaCl–10mM Tris–1.0 mM

EDTA solution (pH 7.4). Electrochemical measurement buffer solution was 10 mM Tris–HCl

solutions (pH 7.0). All oligonucleotides solutions were diluted with corresponding buffer solutions.

All chemicals were analytical grade and sterilized Milli-Q water (18 MΩ/cm) was used in all

experiments.

Table S1 Details of the DNA sequences

Capture probe (Cp)	5′-HS-AAAAGATCAAAgAACAAAGCAAAAA-3′
Assisted probe 1 (Ap1)	5′-GAAATCCATTTGATC-3′-Ferrocene
Assisted probe 2 (Ap2)	5′-TGCTTTGTTCTGGATTTC$GC^LAG^LGT^L$-3′
	(The toeholds are bolded and italicized, L: 2′-O,4′-C-methylene-
	(D-ribofuranosyl)
	nucleotides LNA)
Target (T, BCRA I-gene fragment)	5′-ACCTGCGAAATCCAGAACAAAGCA-3′
Single mismatch Target (T1)	5′-ACCT**A**CGAAATCCAGAACAAAGCA-3′
Single mismatch Target (T2)	5′-ACCT**T**CGAAATCCAGAACAAAGCA-3′
Single mismatch Target (T3)	5′-ACCT**C**CGAAATCCAGAACAAAGCA-3′
Two mismatch Target(2MT)	5′-ACC**A**GCGAAA**A**CCAGAACAAAGCA-3′
Noncomplimentary target (NC)	5′-TGGATGATTTAGATCTTACCCAGT-3′

The underlined bold letters indicate the mismatched position.

Electrochemical measurements. The electrochemical impedance spectra (EIS) and cyclic

voltammogram (CV) measurements were carried out with CHI 660D electrochemical system

(Shanghai Chenhua Equipments, China). The ECL detection system consisted of a BPCL-GP15-TGC ultra-weak luminescence analyzer (Institute of Biophysics, Chinese Academy of Science, Beijing, China), collecting ECL signal system controlled by a personal computer with BPCL program (Institute of Biophysics, Chinese Academy of Science) and a CHI 660D electrochemical system. The electrochemical system consisted of a working electrode (a gold disk electrode modified with DNA probe), a platinum wire as the auxiliary electrode, and a reference electrode (Ag/AgCl). A glass cell with optically flat bottom was used as detection cell. The electrochemical cell was placed directly on the photomultiplier (PMT operated at 1050 V) and the PMT window was only opened towards the working electrode for reducing the interference of ECL from the auxiliary electrode.

CV was carried out in 10 mM Tris-HCl-10 mM $[Fe(CN)_6]^{3-/4-}$ and 10 mM Tris-HCl 10 μM RuHex solution (pH 7.0) at a scan rate of 100 mV/s in the potential range between -0.2 and +0.8 V, -0.5 and +0.1 V, respectively. EIS was measured in 0.1 M KCl–10 mM Tris–HCl–10 mM $[Fe(CN)_6]^{3-/4-}$ solution (pH 7.0) in the frequency range of $0.1\text{-}10^5$ Hz. A Nyquist plot (Z_{re} vs Z_{im}) was drawn to analyze the impedance results. Perform chronocoulometry (CC) with the following parameters: initial potential: 0.2 V; final potential: -0.5 V; number of steps: 2; pulse width: 0.25 s; sample interval: 0.002; sensitivity (C or A/V): $5e^{-5}$ A/V.

Preparation of Ru(bpy)$_3$$^{2+}$–AuNPs composite. AuNPs with a diameter of 16 nm were prepared by citrate reduction of HAuCl$_4$ in aqueous solution according to the literature.[1] In brief, 100 mL of 0.01 % HAuCl$_4$ solution was brought to reflux, and then 3.5 mL of 1 % sodium citrate solution was introduced with stirring. The whole solution was kept boiling for 30 min and cooled to room temperature. The product (AuNPs solution) was stored in a dark glass bottle at 4 °C for

further use. The Ru(bpy)$_3^{2+}$–AuNPs composite was prepared according to the literature.[2] In brief, 150 μL of 40 mM Ru(bpy)$_3^{2+}$ aqueous solution was added into 20 mL of above AuNPs solution under vigorous stirring at room temperature. Several minutes later, a large amount of black precipitate (Ru(bpy)$_3^{2+}$–AuNPs composite) was formed. The resulting Ru(bpy)$_3^{2+}$–AuNPs composite was collected by centrifugation, and then was washed several times with water and suspended in water again.

Preparation of Ru(bpy)$_3^{2+}$–AuNPs modified gold electrode. A GE (2mm in diameter) was cleaned following the reported protocol.[3] The GE was firstly polished with 1.0, 0.3 and 0.05 μM alumina powder respectively, followed by sonication in ethanol and water for 5 min respectively. Then, the GE was electrochemically cleaned in fresh 0.5 M H$_2$SO$_4$ solution to remove any remaining impurities.[3]

The pretreated GE was rinsed with water again. After being dried with nitrogen gas, the GE was soaked in 0.1 M cysteamine aqueous solution for 2 h at room temperature to form the cysteamine monolayer (cysteamine-derivatized GE). After that, the electrode was thoroughly rinsed with water to remove the physically adsorbed cysteamine, and a 2.5 μL of the suspension of Ru(bpy)$_3^{2+}$–AuNPs composite was placed on the cysteamine-derivatized GE surface. The GE was then air-dried at room temperature. After being rinsed with water thoroughly, the luminescent substrate of Ru(bpy)$_3^{2+}$–AuNPs was immobilized on the GE surface. The Ru(bpy)$_3^{2+}$–AuNPs modified GE was immediately used for DNA immobilization and hybridization.

Formation of quenching monolayer of junction-probe-Ru(bpy)$_3^{2+}$–AuNPs on GE surface. Firstly, Ru(bpy)$_3^{2+}$–AuNPs modified GE was modified with a drop of 2.5 μL 1 μM Cp DNA solution for 1 h at room temperature. After being rinsed and dried gently, the Cp–

Ru(bpy)$_3^{2+}$–AuNPs modified GE was further treated with 1 mM MCH for 40 min to cover the spare room of electrode surface and to obtain well-aligned DNA monolayer. Then, 2.5 μL of 10 μM hybridization solution, the solution that Ap1 hybridized with Ap2 for 1h at room temperature, was placed on the DNA self-assembly monolayer (SAM) of MCH/Cp–Ru(bpy)$_3^{2+}$–AuNPs modified GE for 1h at room temperature. After incubation, the DNA modified GE was rinsed with water and dried under a stream of nitrogen gas for preparation, thus a quenching monolayer of junction–probe–Ru(bpy)$_3^{2+}$–AuNPs was formed on the surface of GE.

ECL measurement. 2.5 μL of different target DNA solution was dropped on the surface of junction-probe-Ru(bpy)$_3^{2+}$–AuNPs modified GE prepared as above. After 1 h incubation at room temperature, the GE was extensively rinsed with water and dried by nitrogen gas to remove the unbound oligonucleotides. An ECL cell with three-electrode system consisted of an above treated GE as the working electrode, an Ag/AgCl as the reference electrode and a platinum wire as auxiliary electrode. CV mode, which with a continuous potential scanning from 0.8 to 1.4 V and a scanning rate of 100 mV/s, was applied to achieve ECL signal in 20 mM PBS (pH 8.7) containing 1.0 mM tri-n-propylamine (TPA, a coreactant for ECL) and 5.0 mM LiClO$_4$. The ECL and CVs curves were recorded simultaneously.

2. RESULTS AND DISCUSSION

Thermostability Characterization of the ECL biosensor. To assure the present TMSDR initiated successfully, T-Ap2 duplex must have higher thermal stability than Y-shape junction structure. Previous studies have demonstrated that melting temperature (T$_m$) is a useful physical property of nucleic acids and gives information about the stability of duplexes in a specified environment. T$_m$ is the temperature at which, under a given set of conditions, double-stranded

DNA is changed (50%) to single-stranded DNA.[4] Therefore, the T_m of T-Ap2 duplex, Y-shape junction structure and T-Ap2 duplex free of LNA modification were investigated. As seen in Fig.S1, the T_m value of T-Ap2 duplex (63.5 ℃, curve a) was greatly higher than that of Y-shape junction structure (48.0 ℃, curve c), indicating higher thermal stability. However, without LNA modification, the analogous T-Ap2 showed a lower T_m value (52.0 ℃, curve b), only 4 ℃ higher than Y-shape junction structure. The results indicated that the T_m of oligonucleotides could be increased by the incorporation of LNA residues into the oligo sequence, which made it possible to trigger a strand displacement reaction more easily. All above results of T_m demonstrated that our biosensor indeed worked as expected.
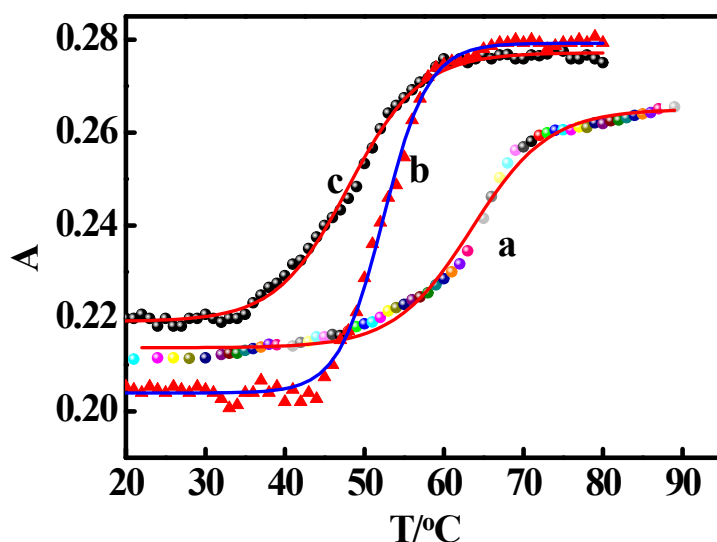

Fig.S1. T_m of T-Ap2 duplex (a), Y-shape junction structure (b) and T-Ap2 duplex free of LNA modification(c)

EIS and CV Characterization of the different stages of the ECL biosensor. In order to confirm the preparing process, EIS of bare GE and different modified GE in a solution of 10 mM $[Fe(CN)_6]^{3-/4-}$ were collected at a potential of 0.21 V (versus Ag/AgCl) in the frequency range of 0.1-10^5 Hz. As shown in Fig. S2, compared with the bare GE (curve a) and Ru(bpy)$_3^{2+}$–AuNPs

modified GE (curve b), the Cp–Ru(bpy)$_3$$^{2+}$–AuNPs modified GE (curve c) showed a larger eT resistance (*Ret*), mainly due to the electrostatic repulsion between negative charges of the DNA backbone and [Fe(CN)$_6$]$^{3-/4-}$. When Cp–Ru(bpy)$_3$$^{2+}$–AuNPs modified GE was incubated in the solutions containing Ap1 and Ap2, junction-probe–Ru(bpy)$_3$$^{2+}$–AuNPs modified GE showed the biggest *Ret* (curve e). This was due to the fact that Cp hybridized with Ap1 and Ap2 to form Y-shape junction structure, and the formation of Y-shape junction structure resulted in a much denser negative charges on the GE surface and generated a much stronger electrostatic repulsion between GE surface and [Fe(CN)$_6$]$^{3-/4-}$. Subsequently, the alternation of the *Ret* in the present of T was investigated. Curve d was the Nyquist plot of [Fe(CN)$_6$]$^{3-/4}$ at the junction-probe–Ru(bpy)$_3$$^{2+}$–AuNPs modified GE after it reacted with T, and it was clearly observed that the *Ret* of curve d was much smaller than that of curve e. This was because the strand displacement reaction triggered by the hybridization of T and LNA modified toehold-mediated lead to the dissociation of the Y-shape junction structure. Thus, with Ap1 and Ap2 dissociated from GE, the decreasing negative charges finally resulted in the decrease of Ret. The corresponding CV curves of the electrodes in the different stage of the biosensor preparation using [Fe(CN)$_6$]$^{3-/4-}$ as the redox probe were shown in the inset of Fig. S2. The results of CVs were consistent with that of EIS, suggesting that our biosensor indeed worked as we expected again.
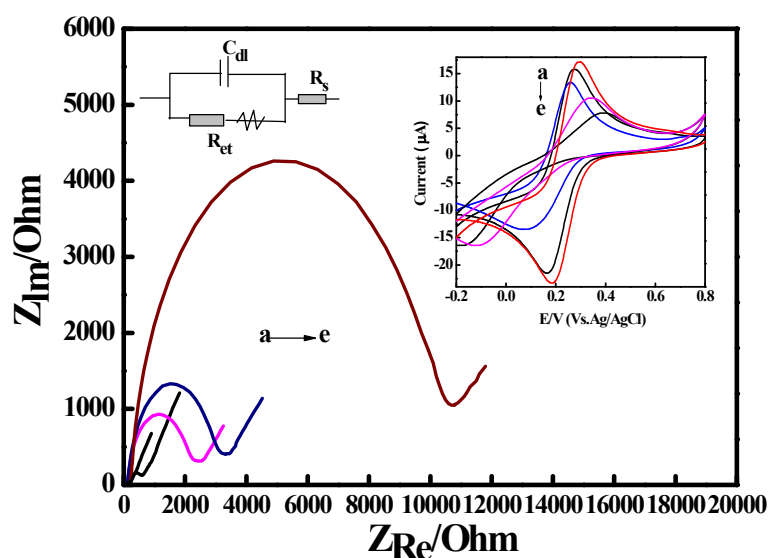
Fig.S2 Nyquist plot of bare GE (a), the Ru(bpy)$_3^{2+}$-AuNPs modified GE (b), the Cp-Ru(bpy)$_3^{2+}$-AuNPs modified GE (c), the junction-probe-Ru(bpy)$_3^{2+}$-AuNPs modified GE   after(d) and before (e) being incubated in the solution containing T. Insert: The corresponding CVs of the electrodes in the different stage of the biosensor preparation. The data were obtained in the presence of 10 mM [Fe(CN)$_6$]$^{4-/3-}$. The biased potential was 0.21 V (versus Ag/AgCl) in the frequency range of 0.1–10^5 Hz and the amplitude was 5.0 mV.

The CC and CV behaviors of RuHex in the different stages of the ECL DNA-modified biosensor. An electroactive complex, RuHex, can be stoichiometrically bound to the anionic phosphate of DNA strands via electrostatic interaction with a cumulative redox charge, which can reflect directly the amount of DNA strands proximal to the electrode surface.[5]

Herein, the CC behaviour of RuHex is employed to interrogate such hybridization events at different stages of the biosensor preparation and measure the time-dependent flow of charge in response to an applied potential step waveform, which is a more reliable and sensitive approach for the detection of surface-confined electroactive species than current-based electrochemical

techniques.[6-7]

The CC of RuHex at different GE surfaces was shown in Fig.S3. As shown in Fig.S3, compared with the bare GE (curve a), the Cp–Ru(bpy)$_3^{2+}$–AuNPs modified GE (curve b) showed a larger CC response (Q), mainly due to the electrostatic binding between negative charges of the DNA backbone and RuHex. After Y-shape junction structure was immobilized on the electrode surface, the signal of CC was increased evidently (curve c), ascribing to the much denser DNA surface density. Nevertheless, in the presence of the T, it triggered the strand displacement reaction, leading to the disassociation of Y-shape junction structure. Therefore less DNA surface density weakened the electrostatic binding with RuHex and resulted in a lower CC signal (curve d).

The CV behaviors of RuHex were also investigated at different stages of the biosensor in order to verify the fabrication of our biosensor, which was shown in the insert of Fig. S3. As shown in curve a, two pair of peaks corresponding to the reduction and oxidation of RuHex could be observed at a relatively dilute concentration at Cp–Ru(bpy)$_3^{2+}$–AuNPs modified GE. Peak 1 indicated that the electron transfer reaction of RuHex at the modified electrode surface was a surface confined redox process since the peak separation was close to zero and peak currents were linearly proportional to scan rates. This pair of peaks was ascribed to RuHex electrostatically binding to the DNA surface, and reflected the amount of DNA on the electrode surface, while peak 2 reflected RuHex diffusion to MCH.[5,8]

When the modified GE was incubated in the solution containing Ap1 and Ap2, Cp would hybridize with Ap1 and Ap2 to form ternary Y-shape junction structure. Therefore, the amount of the RuHex electrostatically binding to the surface of GE increased, resulting in a bigger redox

signal in electrochemical measurement and there was barely a diffusion-controlled peak (curve b).

In the presence of T, it triggered the strand displacement reaction, leading to the disassociation of

Y-shape junction structure. As a result, the amount of the RuHex electrostatically binding to the

surface of GE decreased, resulting in an obviously lower redox signal in electrochemical

measurement (curve c). These above results were paralleled to that of $[Fe(CN)_6]^{3-/4}$, indicating that

our biosensor indeed worked as expected.

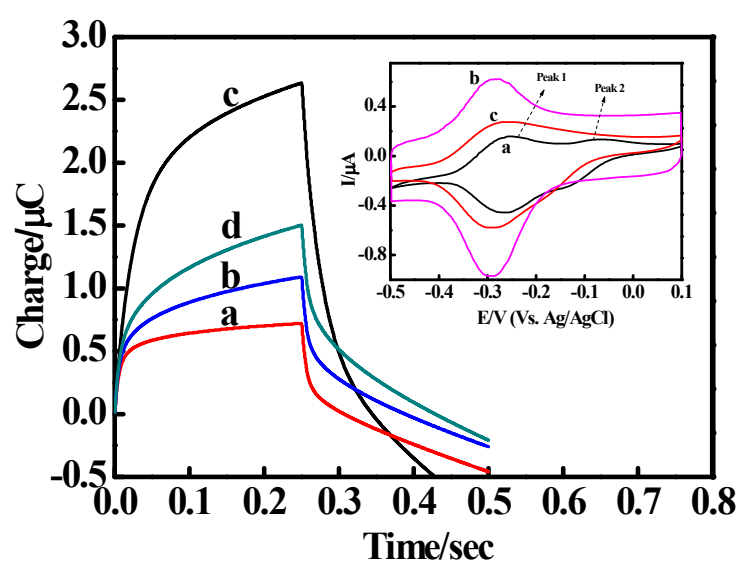**Fig.S3** CC curves of bare GE (a), the Cp-Ru(bpy)$_3^{2+}$-AuNPs modified GE (b), the junction-

probe-Ru(bpy)$_3^{2+}$-AuNPs modified GE (c), and the junction-probe-Ru(bpy)$_3^{2+}$-AuNPs modified

GE   after being incubated in the solution containing T (d). Insert: CVs for a 10 mM Tris–HCl

buffer (pH 7.4) containing 10 μM RuHex obtained at the Cp-Ru(bpy)$_3^{2+}$-AuNPs modified GE (a),

the junction-probe-Ru(bpy)$_3^{2+}$-AuNPs modified GE (b), and the junction-probe-Ru(bpy)$_3^{2+}$-

AuNPs modified GE after being incubated in the solution containing T (c) .

ECL characterization of the different stage of the biosensor. The present ECL biosensor

was also characterized by ECL to demonstrate the modification process further. The

corresponding ECL intensity versus time curves of the different stage of the biosensor were presented in Fig.S4A. As shown in Fig.S4A, no ECL signal could be found for the bare GE (curve a), while the $Ru(bpy)_3^{2+}$-AuNPs modified GE showed an obvious increase due to the extraordinary ECL activity of $Ru(bpy)_3^{2+}$ (curve b). Compared with the $Ru(bpy)_3^{2+}$-AuNPs modified GE, the Cp–$Ru(bpy)_3^{2+}$–AuNPs modified GE (curve c) showed a lower ECL signal, which mainly because the binding of TPA to $Ru(bpy)_3^{2+}$ was hindered by the spatial restriction of DNA self assembly monolayer. The above observation was consistent with the results obtained in the our previous report.[9] When the Cp-$Ru(bpy)_3^{2+}$-AuNPs modified GE was incubated in the solutions containing Ap1 and Ap2, Cp brought Ap1 and Ap2 to form Y-shape junction conformation structure, so the Fc group were close to $Ru(bpy)_3^{2+}$-AuNPs. As shown in curve d of Fig.S4A, ECL intensity was quenched by 98.9 % from 3219 to 36 (curve c). The ultrahigh quenching efficiency would be ascribed to two reason: the first one had been reported as the bimolecular energy and electron transfer between $Ru(bpy)_3^{2+}$ and the oxidized species of Fc, ferrocerium (Fc^+), along with suppression of radical reactions.[2, 10] The second one was steric/conformational effects. The binding of TPA (a co-reactant for ECL) to $Ru(bpy)_3^{2+}$ was hindered due to spatial restriction of the Y-shape junction configuration at such junction-probe-$Ru(bpy)_3^{2+}$-AuNPs modified electrode surface. For the above two reason, the ECL sensor we described here had very low background signal.

When the junction probe-$Ru(bpy)_3^{2+}$-AuNPs GE was incubated in T, Ap2 with a LNA modified single-strand overhang toehold could hybridize with the complementary T and trigger the strand displacement, eventually resulting in the release of the Ap1 tagged with Fc from the modified GE. Thus, without the quenching effect of Fc and the spatial restriction of the Y-shape junction

configuration, the ECL intensity was significantly enhanced (curve e). The recovery of ECL signal

provided a sensing platform for quantitative detection of T. It was worth noting that, the ECL

intensity kept no change even after continuous potential scanning (see Fig.S4B), indicating that

the $Ru(bpy)_3^{2+}$-AuNPs composite immobilized on the GE was very stable. In a word, ECL

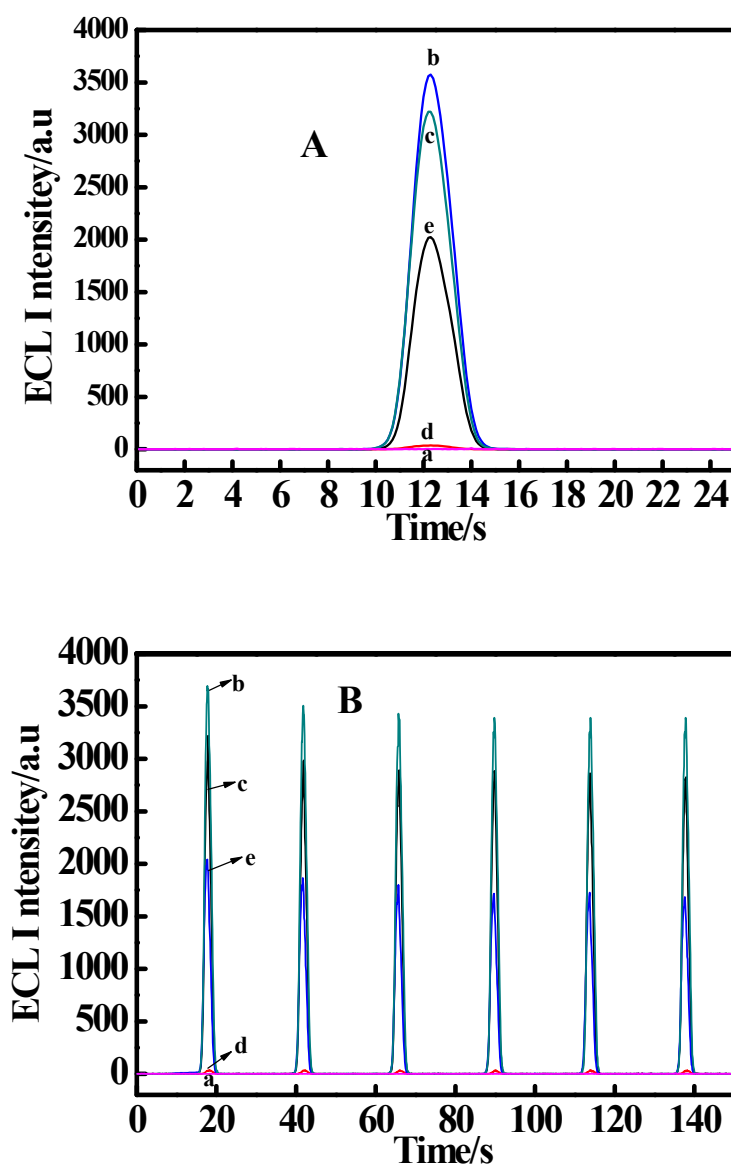experiments further indicated that our biosensor indeed worked as we expected.

Fig.S4 (A) ECL intensity vs. time curves for the bare GE (a), $Ru(bpy)_3{}^{2+}$-AuNPs modified GE

(b), Cp-$Ru(bpy)_3^{2+}$-AuNPs modified GE (c), junction probe-$Ru(bpy)_3^{2+}$-AuNPs modified GE

before(d) and after incubated in 500 fM T(e). (B) Stability of the electrodes under continuous CVs for six cycles. ECL curves were measured in 20 mM PBS containing 1.0 mM TPA and 5.0 mM LiClO$_4$ (pH 8.7).

Label-free detection of T based on EIS. As known, EIS becomes increasingly popular in the field of electrochemical measurements and biosensing applications. Compared to other electrochemical methods, this method is of high sensitivity, signal quantification ease, and ability to separate the surface binding events from the solution impedance. In comparison to CV or differential pulse voltammetry (DPV), which are also used to characterize molecular interactions on the surface of electrodes, EIS is less harmful to the interactions to be examined. Therefore, we apply EIS in the development of a label-free analogic sensor to detect T.

As illustrated in the Fig.S5A, in the absence of T, Cp, Ap1 and Ap2 will hybridize to form a ternary Y-shape junction structure on the surface of GE (junction-probe–GE). In this scenario, these negatively charged junction-probes are immobilized on the electrode surface, leading to the reducing response of $[Fe(CN)_6]^{3-/4-}$ anions and the enhancing electron-transfer resistance. Whereas, in the presence of T, strand displacement reaction triggered by the hybridization of T and LNA modified toehold-mediated lead to the dissociation of the Y-shape junction structure as well as the decrease of Ret.

Under the optimum conditions, the relationship between the Ret value and the concentrations of T was studied. Fig.S5B shows the Ret value of Nyquist plots decrease with the increasing concentrations of T. It is also found that ΔRet (the change of Ret) has a relationship with the concentrations of T in the range of 0.5-2.0 nM (inset of Fig.S5B). The regression equation is Y= 3141.07X-2019.78, r= 0.9938, where Y is the ΔRet, X is the concentration of T, r

is the regression coefficient. The detection limit of this method is 62 pM (defined as S/N=3). Therefore, using this sensing platform, a simple, rapid, highly sensitive electrochemical biosensor for the detection of T can be developed. However, the method suffers from many kinds of nonspecific impedance changes, including initial electrode contamination, repetitive measurements, additional CV or DPV measurements, and additional incubations in the buffer between measurements. The potential drawbacks of the method can result in false-positive or false-negative results. Therefore, we herein demonstrate a new method based on ECL for the detection, whose principle was mentioned in the beginning, and it provides a good way without the disadvantages mentioned above.
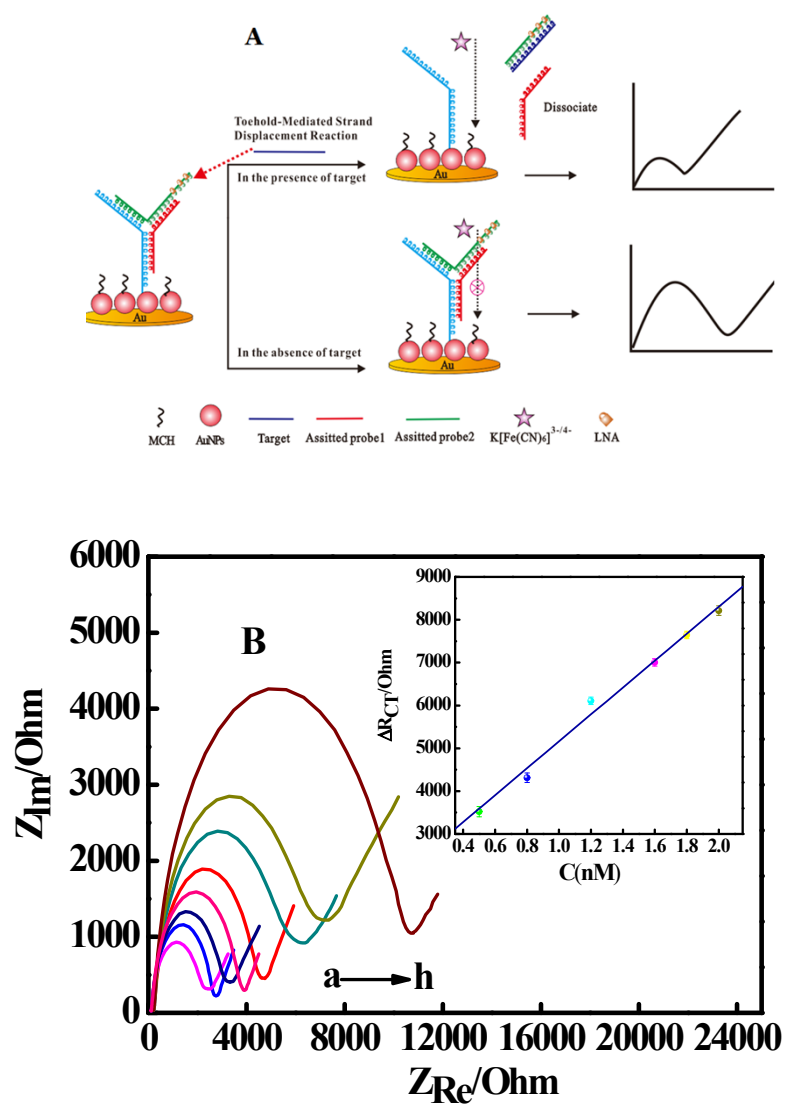
Fig.S5 (A) Experimental principle of the EIS biosensor. (B) Nyquist plot of the Cp-Ru(bpy)$_3^{2+}$-AuNPs modified GE (a), the junction-probe-Ru(bpy)$_3^{2+}$-AuNPs modified GE after interaction of different concentrations of different T(from b to h): 2.0 nM, 1.8 nM, 1.6 nM, 1.2 nM, 0.8 nM, 0.5 nM, 0 nM. Insert: The linear relationship between impedance and the target concentration. The data were obtained in the presence of 10 mM [Fe(CN)$_6$]$^{4-/3-}$. The biased potential was 0.21 V (versus Ag/AgCl) in the frequency range of 0.1–10^5 Hz and the amplitude was 5.0 mV.

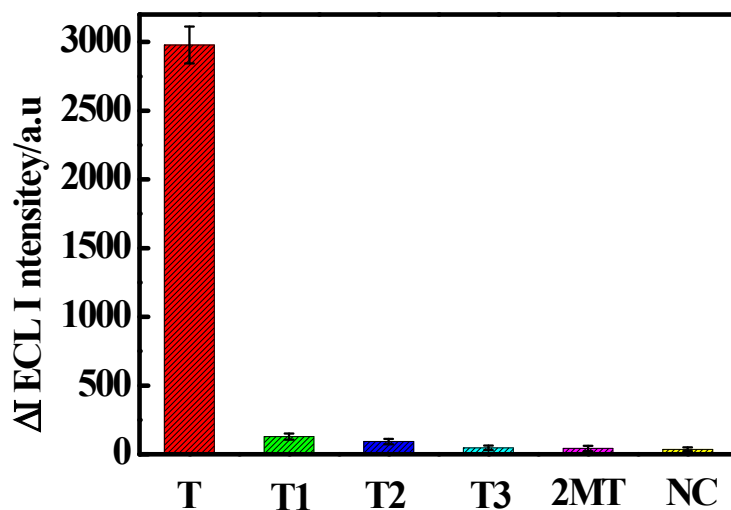**The selectivity of the toehold-mediated junction-probe ECL biosensor.**

Fig.S6 ECL intensity on junction-probe-Ru(bpy)$_3$ $^{2+}$-AuNPs modified GE after it reacted with T and other control DNA. Each concentration of DNA samples is 800 fM. ECL experiments were measured in 20 mM PBS containing 1.0 mM TPA and 5.0 mM LiClO$_4$ (pH 8.7).

Detection of artificial cells sample. In order to evaluate the practical applicability, the proposed biosensor was used for determining the recoveries by dissolving three different concentrations of T into HeLa Cells Lysate. HeLa Cells Lysate was prepared as described previously with some slight modification.[11] Briefly, the incubated cells were collected by trypsinization and centrifugation, washed with PBS, and pelleted at 3000 rpm for 5 min at 4 °C.

After being resuspended in RIPA cell lysis solution (from Thermo Scientific) and incubated for 30 min at -20 °C, the cells were centrifuged at 12000 rpm for 30 min at 4 °C. Finally, the supernatant was collected and filtered by 0.45 μm filter membrane prior to store at -20 °C. As shown in Table S2, for 5-fold diluted lysate sample, the obtained recoveries were between 93.8 and 96.8 % (n=5). The results prove that the biosensor has potential for biological sample analysis.

Table S2 Determination of T in artificial cell sample (n=5)

T added (fM)	Detected by this method (fM)	Recovery of this method (%)	RSD (%)
200	189	94.5	6.9
400	387	96.8	6.7
600	563	93.8	5.6

References

1 Doron, A., Katz, E., Willner, I. Langmuir. 1995, **11**, 1313.

2 Wang, X. Y., Yun, W., Dong, P., Zhou, J. M., He, P. G., Fang, Y. Z. Langmuir. 2008, **24**, 2200.

3 Fan, C., Plaxco, K. W., Heeger, A. J., Proc. Natl. Acad. Sci. U.S.A. 2003, **100**, 9134.

4 Richard, O. Biophys. Chem. 2005, **117**, 207.

5 Lao, R., Song, S., Wu, H., Wang, L., Zhang, Z., He, L., Fan, C. Anal. Chem. 2005, **77**, 6475.

6 Zhang, J., Song, S., Wang, L., Pan, D., Fan, C. Nat. Protoc. 2007, **2**, 2888.

7 Zhang, J., Song, S., Zhang, L., Wang, L., Wu, H., Pan, D., Fan, C. J. Am. Chem. Soc. 2006, **128**, 8575.

8 Fan, Q., Zhao, J., Li, H., Zhu, L., Li, G. X. Biosens. Bioelectron. 2012, **33**, 211.

9 Zhang, J., Chen, P. P., Wu, X. Y., Chen, J. H., Xu, L. J., Chen, G. N., Fu, F. F. Biosens.

Bioelectron. 2011, **26**, 2645.

10 Cao, W., Ferrance, J. P., Demas, J., Landers, J. P. J. Am. Chem. Soc. 2006, **128**, 7572.

11 Wang, D. Z.; Tang, W.; Wu, X. J.; Wang, X. Y.; Chen, G. J.; Chen, Q.; Li, N.; Liu, F. *Anal.*

Chem. **2012**, *84*, 7008.